

## Influence of Constant Magnetic Field on Electrodeposition of CoW/Cu/CoW Composite

Marta Jaksender, Ewa Miękoś, Marek Zieliński\*, Karina Kolodziejczyk, Dariusz Sroczyński, Anna Łukawska, Dominik Szczukocki, Barbara Krawczyk, Karolina Czarny, Renata Juszczyk

Department of Inorganic and Analytical Chemistry, Faculty of Chemistry, University of Lodz, Tamka 12, 91-403 Lodz, Poland

\*E-mail: [zielmark@chemia.uni.lodz.pl](mailto:zielmark@chemia.uni.lodz.pl)

Received: 22 July 2017 / Accepted: 1 March 2018 / Published: 5 June 2018

---

Magnetic field influences the process of electrolytic deposition of materials, including metal composites. Numerous studies have shown that the magnetic field interferes in the rate of deposition, surface morphology, corrosion resistance, and hardness of the obtained coatings. The purpose of the study was to investigate the effect of a constant magnetic field on the processes of electrodeposition of the gradient metallic composite CoW/ Cu/CoW, and to compare the morphology of the surface of the composite obtained in and without the involvement of a constant magnetic field. Another step to achieve the objectives was to study the giant magnetoresistance (GMR) phenomenon, involving a change in the material resistance occurring in gradient metallic composites exposed to an external magnetic field. The percentage changes of resistance in constant magnetic field of magnetic induction  $B = 1\text{T}$  were estimated for CoW/Cu/CoW composite as well as for a reference composite Fe/Cr/Fe, known from the literature.

---

**Keywords:** Constant magnetic field (CMF), Electrodeposition, Composites, Lorentz force, Giant magnetoresistance (GMR)

### 1. INTRODUCTION

The control of processes of obtaining materials is the object of interest of contemporary materials engineering and applied electrochemistry. The justification for those tendencies is a possibility to obtain materials that are characterized by unusual properties. The electrochemical deposition method provides an additional technique allowing to obtain composite layers characterized by broad technological applicability. It is an economical option as compared to other techniques, and also a convenient way to form a thin film of metallic structures. Electrochemical method for preparing graded materials, including materials known as superlattices, can be an alternative to other methods by

which such materials can be obtained (i.e. Molecular Beam Epitaxy, Cathodic Sputtering, Metal Organic Chemical Vapor Deposition) [1]. The properties of the deposited coatings are dependent on the parameters of the deposition process, i.e. composition of the galvanic bath, deposition techniques, pH, and temperature of the solution, concentration as well as the type of current and its density [2]. Electrochemical method allows to control the deposition rate of the material and its chemical composition. Various studies show clearly that electrodeposition is a useful method for the preparation of a number of multilayer composites, such as Ni/Cu, CoNi/Cu, CoCu/Cu, NiFe/Cu [3-5]. Metallic multilayers are obtained using two electrochemical methods. In both methods, the multilayer is made from a solution containing metal ions forming the alternating layers. The difference lies in modulation of the current or potential during the deposition process. Deposition of alternating layers of two metals is carried out by changing the current or potential. This is due to a large difference between the ion concentration of the more noble metal and the ion concentration of the less noble metal. The use of electrochemical metal deposition technique from one solution is possible when the position of a number of metals in voltage is significantly different. This difference enables the deposition of the more noble metal layers, dia- or paramagnetic (Cu, Ag, Au) at a higher potential, alternated layers of a less noble metal, or a ferromagnetic or its alloys (Co, Ni, NiCo) at a lower potential. Obtaining a material from various electrolytes allows to produce a material with almost pure metal layers, in contrast to a material obtained from one electrolyte (by changing the current-potential conditions). The essence of the latter technique is the appropriate selection of the potentials applied to the working electrode, and control of the electric charge flow during the deposition of a single layer. Applying a sufficiently low potential to the electrode will reduce both the more noble and the less noble metal ions. In contrast, applying a higher deposition potential is determined to reduce the more noble metal ion only. The solutions used to deposit layers are characterized by a relatively high concentration of the less noble metal ions in comparison with the concentration of noble metal ions. Therefore, reduction of the less noble metal ions is limited by kinetics of the reaction, whereas reduction of noble metal ions is limited by diffusion to the electrode surface. The deposited layer with lower potential dominant component is the less noble metal. However, this layer also contains a small amount (up to 10%) of the more noble metal [6]. The object of the study was the metallic gradient composite with a CoW/Cu/CoW symbol. Deposition of alternating ferromagnetic layers (CoW) and the diamagnetic layer (Cu) yields a material with new and specific magnetic characteristics. Tungsten is a metal which is unable to settle isolated from the aqueous salt solution. There is, however, codeposition of the metal from the ferrous metals group Fe, Ni, Co [7]. The CoW alloy is characterized by high corrosion resistance, hardness and durability [8]. These properties have been the reason for a clear interest in the selected alloy. Furthermore, the electrolytic deposition of metals and alloys of the ferrous group is of interest because of their magnetic properties [9-10]. The magnetic properties of the deposited layers of CoW are used for recording data on high density data storage devices, and magneto. Materials with magnetic application capabilities should have additional functional features, including, among others, corrosion resistance and durability at high temperatures. The deposited CoW alloy layer fully meets the technological requirements [11]. Another parameter that changes the characteristics of the process of electrolytic deposition of metals, alloys, metallic composites environment is constant magnetic field. The influence of magnetic field on the course of basic electrochemical processes has been actively

studied in recent times [12]. Research shows that the magnetic field interferes in the deposition rate, surface morphology, corrosion resistance, and hardness of the resultant coatings. The effect of magnetic field on the processes taking place in the electrochemical cells is generation of Lorentz force ( $F_L$ ), which is obtained by multiplying the magnetic induction vector ( $B$ ) and current density ( $j$ ). The Lorentz force causes convective flow, the consequence of which is the change of electrodeposition rate, surface morphology of the deposited layers and corrosion resistance [13]. Investigation of the effect of changes in the magnetic field inducing the process of electrodeposition of CoFe layers demonstrated that a magnetic field with its direction parallel to the induction electrode surface increases the rate of layers deposition and electrical current density [12]. It has been shown that NiFe, CoMo, CoW, CoMoW electrodeposited in a magnetic field characterized by a smoother surface and uniform structure [7, 14-19]. The observed changes are attributed to the effect of magnetohydrodynamics (MHD), the main driving force of which is the Lorentz force. This causes the electrolyte to increase the mass transport in the vicinity of the electrode. It was also found that an increase in current density under constant magnetic field (CMF) is caused by a decrease in the thickness of the diffusion layer ( $\delta_D$ ) [20-22]. The consequence of this is an increase in electroactive particle concentration near the electrode and thus the weight of the deposited layer.

## 2. EXPERIMENTAL

Electrochemical measurements using the CV method were performed in an electrochemical cell, with a three-electrode system. The circuit consisted of: a working electrode (gold disk) with an area of  $0.1017 \text{ cm}^2$ , auxiliary electrode (platinum mesh) and a reference electrode (saturated calomel). Electrochemical processes were controlled by the ATLAS CORR 05 computer program using the Atlas 0531 type Electrochemical Unit & Impedance Analyzer potentiostat. The surface of the working electrode was cleaned mechanically (using grit 2000 sandpaper), chemically (using a chromic acid cleaning mixture) and electrochemically (polarization in a stock solution of  $0.1 \text{ M H}_2\text{SO}_4$ , within the potential range from  $-2\text{V}$  to  $+2\text{V}$ ). The electrochemical method for obtaining gradient materials, including also the so-called superlattice materials, may provide an alternative for obtaining such materials with other methods. Co-W / Cu / Co-W composite was obtained in two ways, using various galvanic solutions. The first method consisted in depositing alternating layers using (interchangeably) Electrolyte IA containing:  $0.2 \text{ M CoSO}_4 \cdot 7\text{H}_2\text{O}$ ,  $0.05 \text{ M Na}_2\text{WO}_4 \cdot 2\text{H}_2\text{O}$ ,  $0.4 \text{ M Na}_3\text{C}_6\text{H}_5\text{O}_7 \cdot 2\text{H}_2\text{O}$ ,  $0.1 \text{ M H}_2\text{SO}_4$ , to deposit the first composite layer (Co-W), and an Electrolyte IB containing:  $0.02 \text{ M CuSO}_4 \cdot 5\text{H}_2\text{O}$ ,  $0.4 \text{ M Na}_3\text{C}_6\text{H}_5\text{O}_7 \cdot 2\text{H}_2\text{O}$ ,  $0.1 \text{ M H}_2\text{SO}_4$ , to deposit a second composite layer (Cu). The second method was to obtain the tested composite using one galvanic bath composition. For this purpose, Electrolyte II, containing:  $0.2 \text{ M CoSO}_4 \cdot 7\text{H}_2\text{O}$ ,  $0.05 \text{ M Na}_2\text{WO}_4 \cdot 2\text{H}_2\text{O}$ ,  $0.02 \text{ M CuSO}_4 \cdot 5\text{H}_2\text{O}$ ,  $0.4 \text{ M Na}_3\text{C}_6\text{H}_5\text{O}_7 \cdot 2\text{H}_2\text{O}$ ,  $0.1 \text{ M H}_2\text{SO}_4$  was used. The alternating metal layers: CoW (alloy)/Cu (metal)/CoW (alloy) were obtained with the sweep rate of  $50 \text{ mV} \cdot \text{s}^{-1}$  and the resulting cathodic current and cathodic potential. Some of the measurements were performed in the environment of a constant magnetic field. It was generated by an ER 2505 laboratory electromagnet. The magnetic induction  $B$ , used in the study within the value range from zero to  $1.0 \text{ T}$ , was directed in parallel to the

surface of the working electrode. Measurements of atomic force microscopy (AFM) were performed using an AFM Dimension Bruker Surface Nano, Tapping type microscope. SEM measurements and analysis of the elemental composition was performed using a Nova NanoSEM 450 (FEI) microscope equipped with an EDS spectrometer.

### 3. RESULTS AND DISCUSSION

#### 3.1. Electrochemical studies using Cyclic Voltammetry

The Au electrodes were prepared according to the procedure described in the experimental section. Measurements are obtained by Cyclic Voltammetry, in order to investigate the effect of the constant magnetic field on the CoW/Cu/CoW composite metal electrodeposition processes. The tested composite was prepared using the technique of electrolytic deposition from Electrolyte I (IA and IB) and Electrolyte II. Electrochemical studies conducted by the CV method had the following parameters predetermined before the composites were obtained and examined: temperature (20 °C), electrochemical deposition time (5 min.), sweep rate 10, 50, 100  $\text{mV} \cdot \text{s}^{-1}$ , and magnetic induction B ranging from 0 to 1 T. Figure 1 shows a selection of cyclic voltammograms obtained during deposition of the individual components of the composite with and without the participation of the magnetic field.

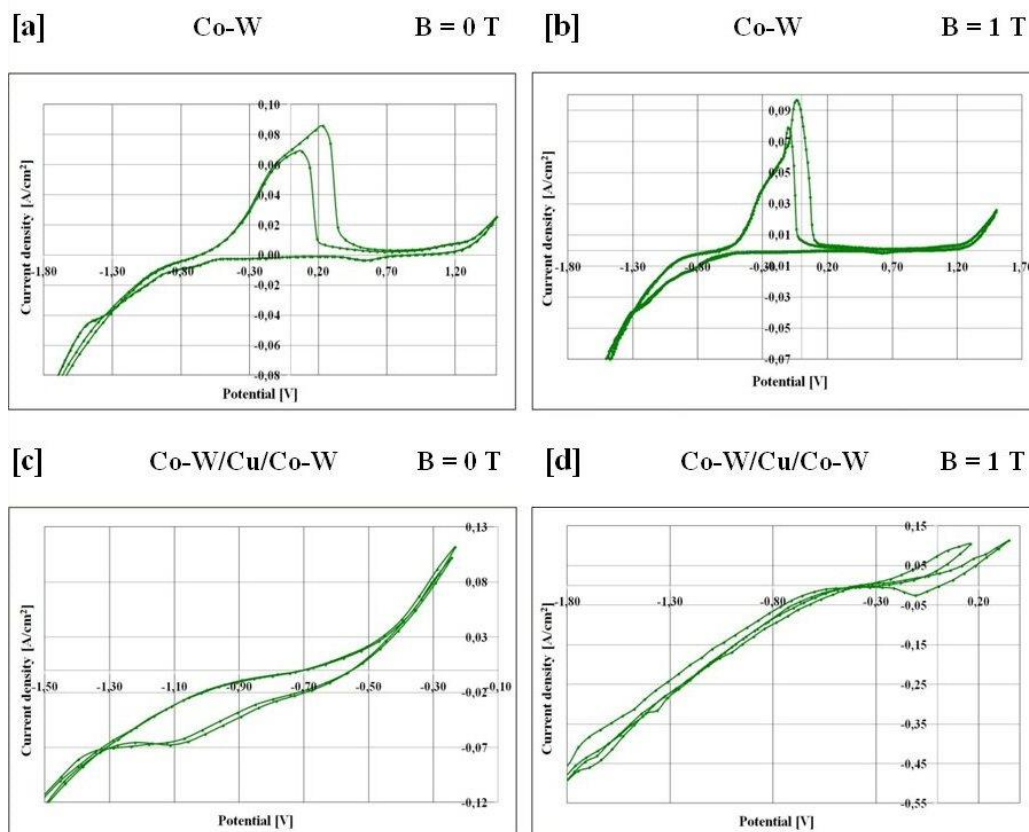


**Figure 1.** Cyclic voltammograms for the individual components of the composite deposited in the absence and within CMF obtained with different electrolytes, for scan rate  $50 \text{ mV} \cdot \text{s}^{-1}$ .

In order to illustrate the influence of CMF ( $B = 1\text{T}$ ), the dependence of anodic oxidation current density of the first composite component (CoW) and the potential have been shown in one graph (Figure 2).

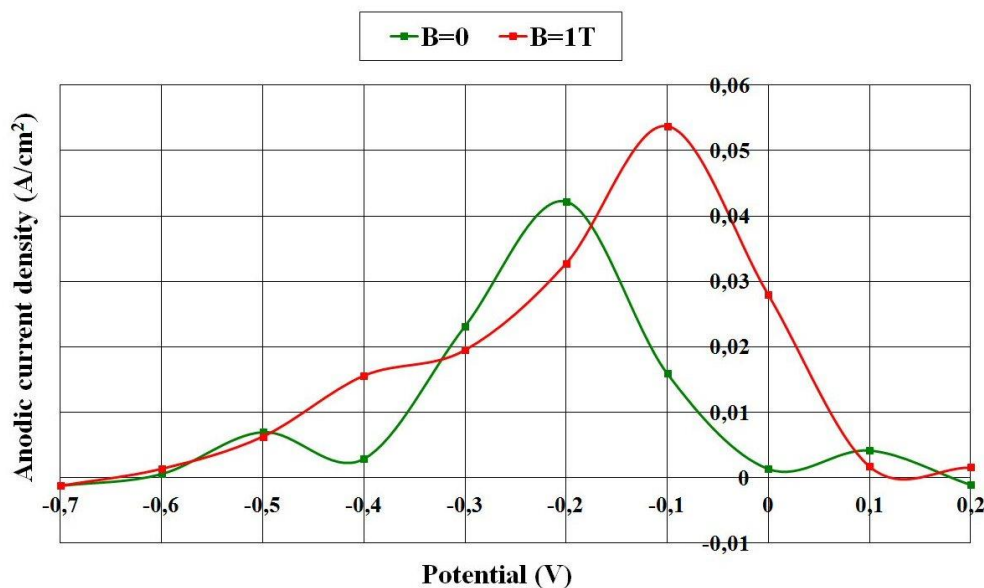


**Figure 2.** Dependence of anodic oxidation current density of CoW alloy on the potential in a CMF and without a CMF, scan rate  $50\text{ mV s}^{-1}$ .

At the selected rate of potential increase ( $50\text{ mV s}^{-1}$ ) in the environment of the constant magnetic field, the value of the anodic current density peak ( $j_a$ ) of CoW alloy oxidation process increases. Under constant magnetic field of magnetic induction  $B = 1\text{ T}$ , the potential of CoW alloy oxidation process ( $U_a$ ) also shifts towards more positive values. The consequence is an increase in potential differences between the Co-W alloy reduction potential ( $U_k$ ) and oxidation potential ( $U_a$ ), i.e. ( $\Delta U$ ). It results in an increase of the degree of irreversibility of the process. By analyzing both the potential and current values of CoW / Cu / CoW composite reduction and oxidation, the difference between the values of cathodic and anodic current density ( $\Delta j$ ) as well as the difference between the cathodic and anodic potentials ( $\Delta U$ ) can be determined (Table 1).

**Table 1.** CV method. Potential and current values of CoW / Cu / CoW composite reduction and oxidation in constant magnetic field ( $B = 1\text{ T}$ ) and in the absence of constant magnetic field.

Metal	Magnetic induction B [T]	Cathodic current density $j_c$ [ $\text{A}\cdot\text{cm}^{-2}$ ]	Cathodic potential $U_c$ [V]	Anodic current density $j_a$ [ $\text{A}\cdot\text{cm}^{-2}$ ]	Anodic potential $U_a$ [V]
Co – W	0	-0.0158	-0.909	0.0427	-0.192
Co – W	1	-0.0264	-1.280	0.0536	-0.116
Cu	0	-0.0761	-1.430	0.0677	0.384
Cu	1	-0.0500	-1.360	0.0547	-0.155

On the basis of the values of potential differences ( $\Delta U$ ) and current density differences ( $\Delta j$ ), correlations with magnetic induction  $B$  can be plotted (Figure 3 and Figure 4). ( $\Delta U$ ) for the diamagnetic (Cu) decreases with an increase of magnetic induction  $B$ , whereas it increases in the case of the ferromagnetic (CoW). Similarly, ( $\Delta j$ ) for the diamagnetic (Cu) also decreases with an increase of magnetic induction  $B$ , and increases for the ferromagnetic (CoW).

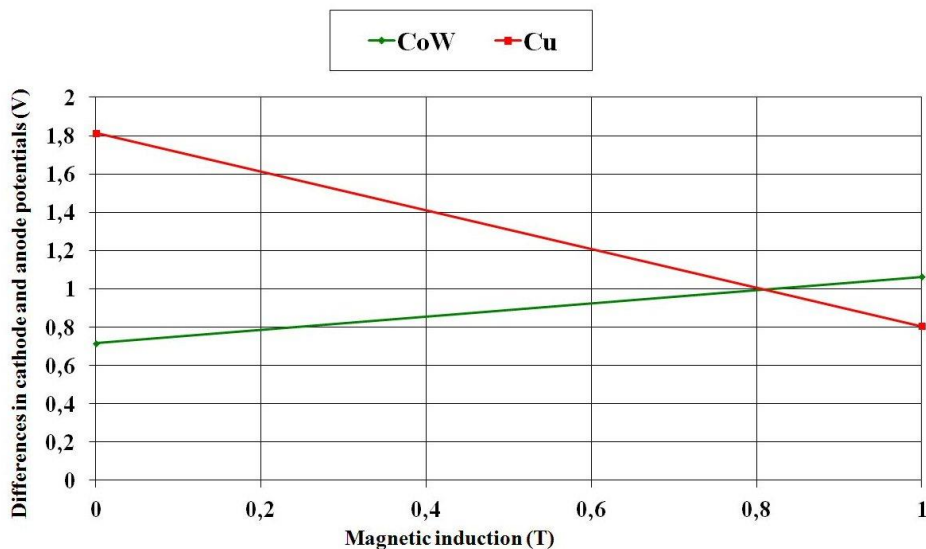


**Figure 3.** Correlation of the difference between cathodic and anodic potentials ( $\Delta U$ ) with magnetic induction ( $B$ ), for the ferromagnetic (CoW) and the diamagnetic (Cu).

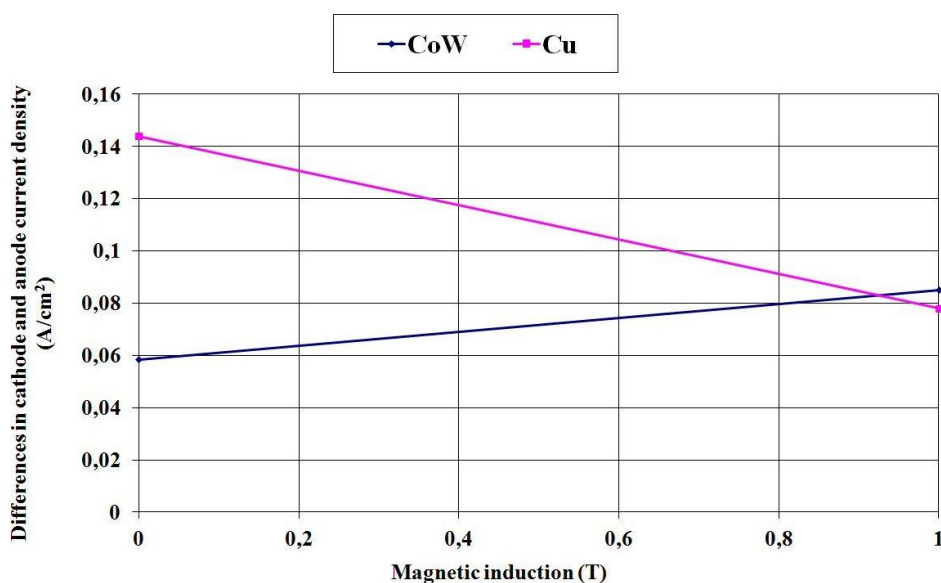


**Figure 4.** Correlation of the difference between cathodic and anodic current densities ( $\Delta j$ ) with magnetic induction ( $B$ ), for the ferromagnetic (CoW) and the diamagnetic (Cu).

On this basis it was noticed that  $\Delta j$  and  $\Delta U$  decreases with increasing magnetic induction for the diamagnetic (Cu), while increasing in the case of the ferromagnetic material (CoW). Electrodeposition in an environment of constant magnetic field has been a phenomenon studied actively over the last few years. Applying a constant magnetic field to the electrode surface increases the mass transport to the surface. This phenomenon is known as the effect of magnetohydrodynamics (MHD), which describes the influence of the applied magnetic field on the electrochemical processes. MHD examines complex systems with a conductive liquid, and the electromagnetic field. In a moving fluid, the induced electric currents interact with the magnetic field with the help of the Lorentz force, which plays a key role due to increasing the convective flow of charged particles. The Lorentz force causes an additional movement of the electrolyte, which in turn leads to the formation of the hydrodynamic Navier - Stokes layer ( $\delta_H$ ), the formation of which is further described in the previous paper. Krause et al. also wrote [23] that: two different effects of a magnetic field  $B$  on the electrodeposition of cobalt have been observed, the MHD effect caused by the Lorentz force and decreasing deposition rates attributed to the action of the paramagnetic force, due to concentration gradients and therefore gradients of the molar susceptibility of the electrolyte close to the surface of the electrode. Much recent work on the influence of magnetic fields acting on currents has been focussed on micro-MHD, where qualitative descriptions of the phenomena have been advanced [22].

Based on the results, an increase in current density under the influence of CMF was noted. Lioubashevski, Katz and Willner presented [24] a theoretical model that shows the influence of magnetic field on the electrochemical processes and dependence of electrical current density values of magnetic induction. The results presented in this study are consistent with the Navier - Stokes equation (1):

$$j = (4.3 \times 10^3) n^{\frac{3}{2}} A^{\frac{3}{4}} D v^{-\frac{1}{4}} C^{\frac{4}{3}} B^{\frac{1}{3}} \quad (1)$$

where:  $j$  - current density,  $n$  - number of electrons participating in the reaction,  $A$  - area of the electrode  $v$  - viscosity of the solution,  $C$  - electroactive ion concentration in the electrolyte  $B$  - magnetic induction.

O'Reilly, Hinds and Coey claimed [20] that the increase in current density under the influence of CMF is due to a decrease in the thickness of the Nernst diffusion layer ( $\delta_D$ ), according to the formula (2):

$$\delta_D \approx 1.59 (\rho R v^{2/3} D^{1/3})^{1/3} (n F C B)^{-1/3} \quad (2)$$

where  $\rho$  - electrolyte density,  $R$  - radius of the working electrode,  $v$  - kinematic viscosity of the electrolyte,  $D$  - electrolyte diffusion,  $n$  - number of electrons involved in the electrochemical process,  $F$  - Faraday's constant,  $C$  - concentration of electroactive ions in the solution and  $B$  - magnetic induction.

Reducing the thickness of the Nernst diffusion layer ( $\delta_D$ ) increases the concentration of electroactive particles at the surface of the electrode, resulting in a greater mass of the deposited layer, according to the formula (3):

$$m \approx 0.63 (\rho R)^{-1/3} v^{-2/9} D^{8/9} (n F C B)^{1/3} \quad (3)$$

where:  $m$  - the mass of the particle.

Ebadi et al. concluded that this is due to the Lorentz force increases with increasing current density [25], due to increased interaction between the magnetic flux and electric current density.

### 3.2. Characteristics of AFM, SEM, EDS

Figures 5 and 6 show the surface morphology of the CoW/Cu/CoW composite obtained Electrolyte I (IA and IB) and Electrolyte II with and without the presence of the constant magnetic field ( $B = 1\text{T}$ ). Based on the AFM images, it was found that the effect of CMF changes the surface morphology of the deposited composite. The CoW/Cu/CoW coatings deposited in a CMF have a smoothed surface. In order to deepen the analysis of surface topography, we obtained SEM images for comparison. Olvera et al. also wrote [26] that: the application of a perpendicular magnetic field during the synthesis modified slightly the morphology of the alloys. In the absence of magnetic field, the  $\text{Co}_x\text{Ni}_{100-x}$  film grows along the (200) direction. However, when the magnetic field was applied, a preferential orientation along the (111) direction was observed.

Figures 7 and 8 show the electrode surface coated with the studied composite obtained from Electrolyte I (IA and IB), as well as from Electrolyte II, and a reference clear (not coated) surface of Au electrodes. SEM images show that the effect of the constant magnetic field increases the resistance to corrosion of the test material, due to reduced stress within the material.

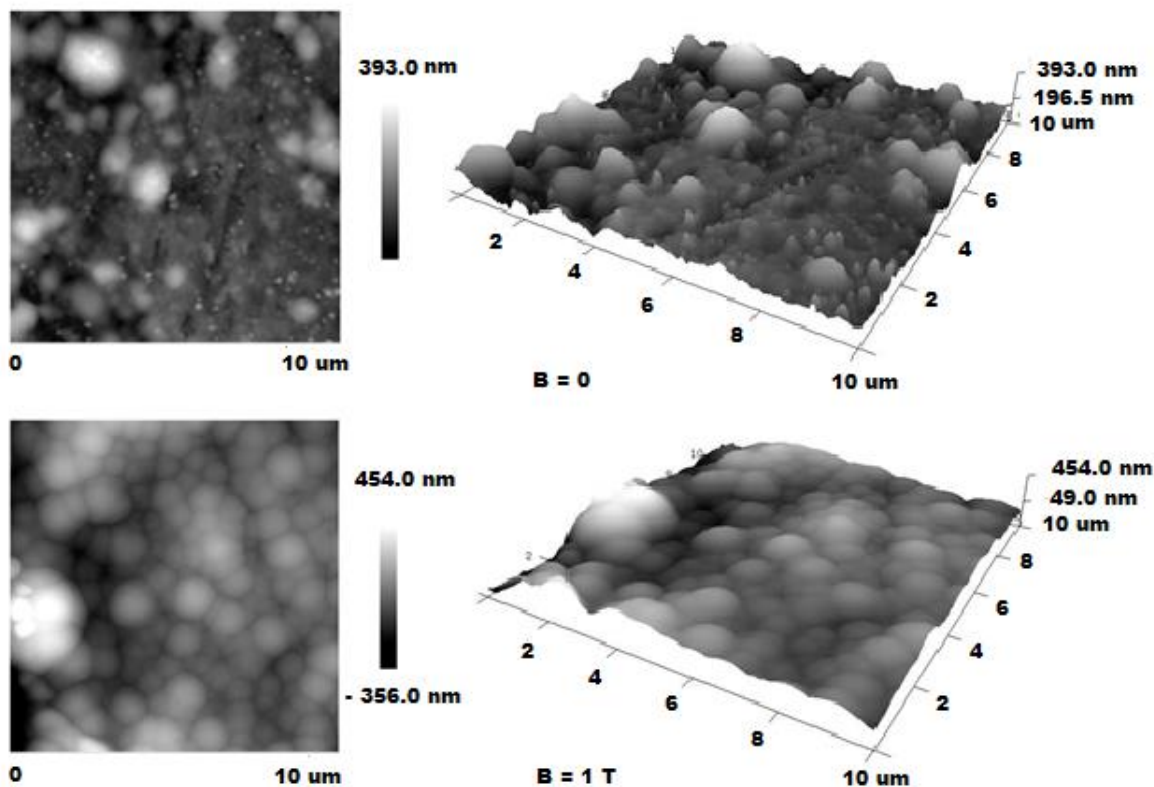


**Figure 5.** AFM images of the CoW/Cu/CoW composite obtained from Electrolyte I (IA and IB), under the influence of CMF.



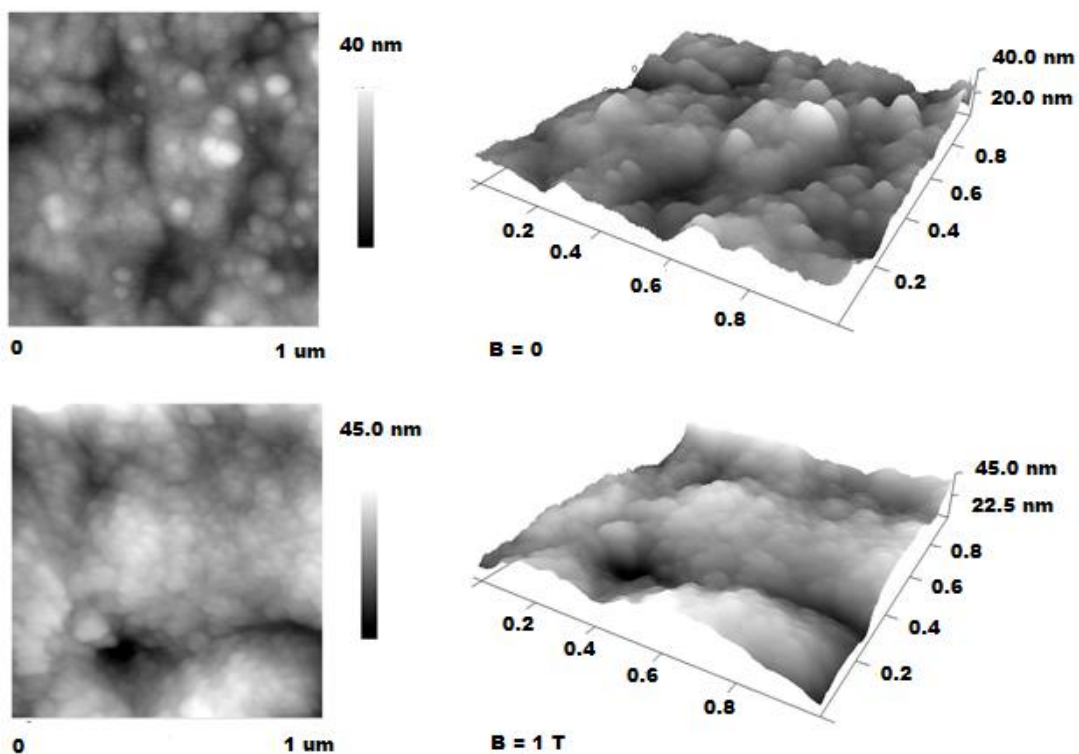


**Figure 6.** AFM images of the CoW/Cu/CoW composite obtained from Electrolyte II, under the influence of CMF.

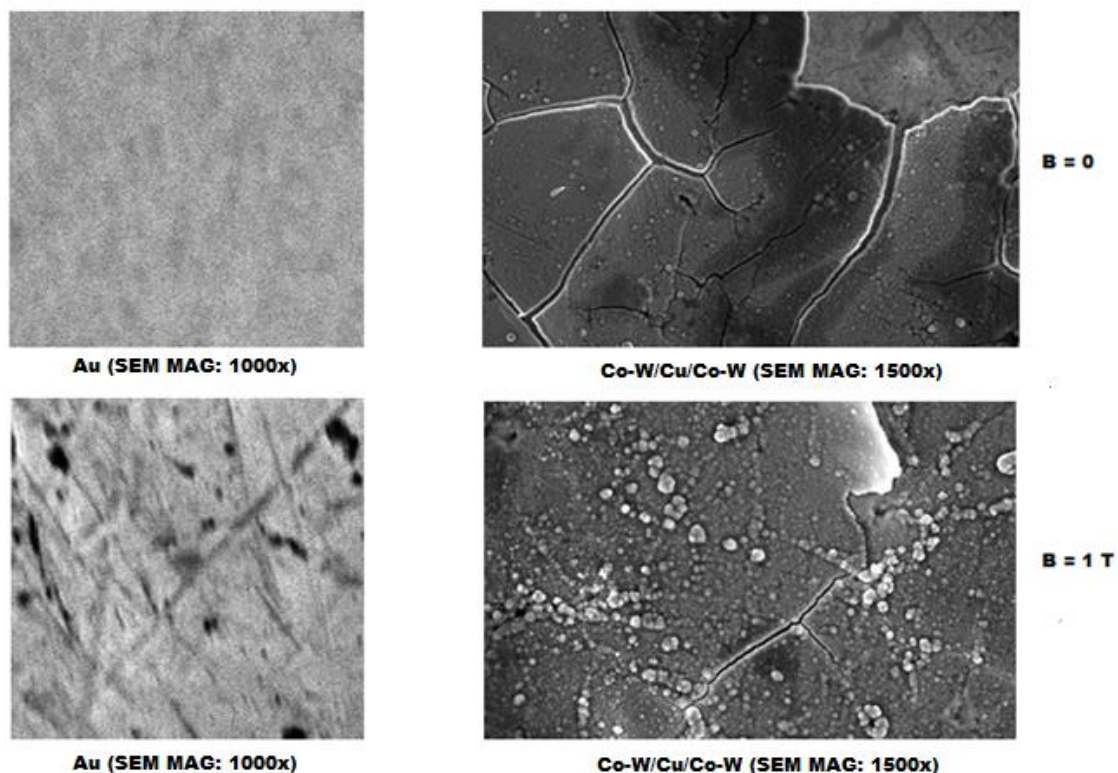


**Figure 7.** SEM images of the CoW/Cu/CoW composite obtained from Electrolyte I (IA and IB) and for uncovered electrode, under the influence of CMF.

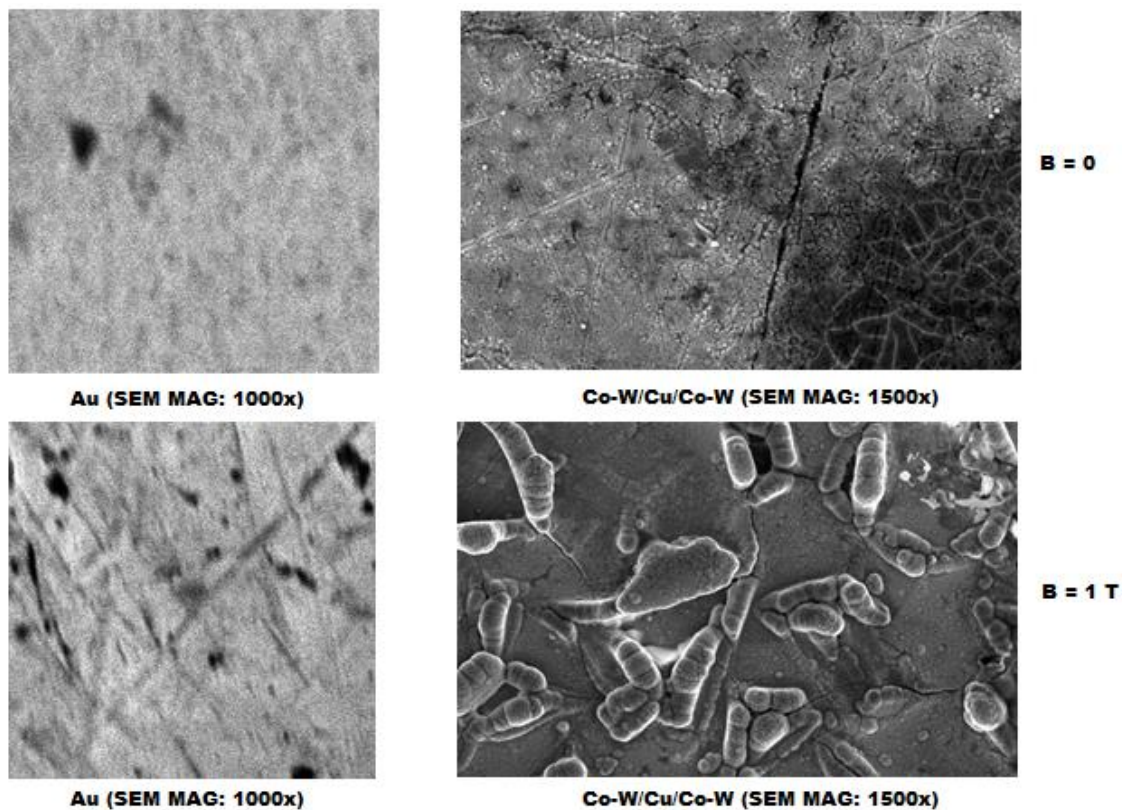


**Figure 8.** SEM images of the CoW/Cu/CoW composite obtained from Electrolyte II and for uncovered electrode, under the influence of CMF.

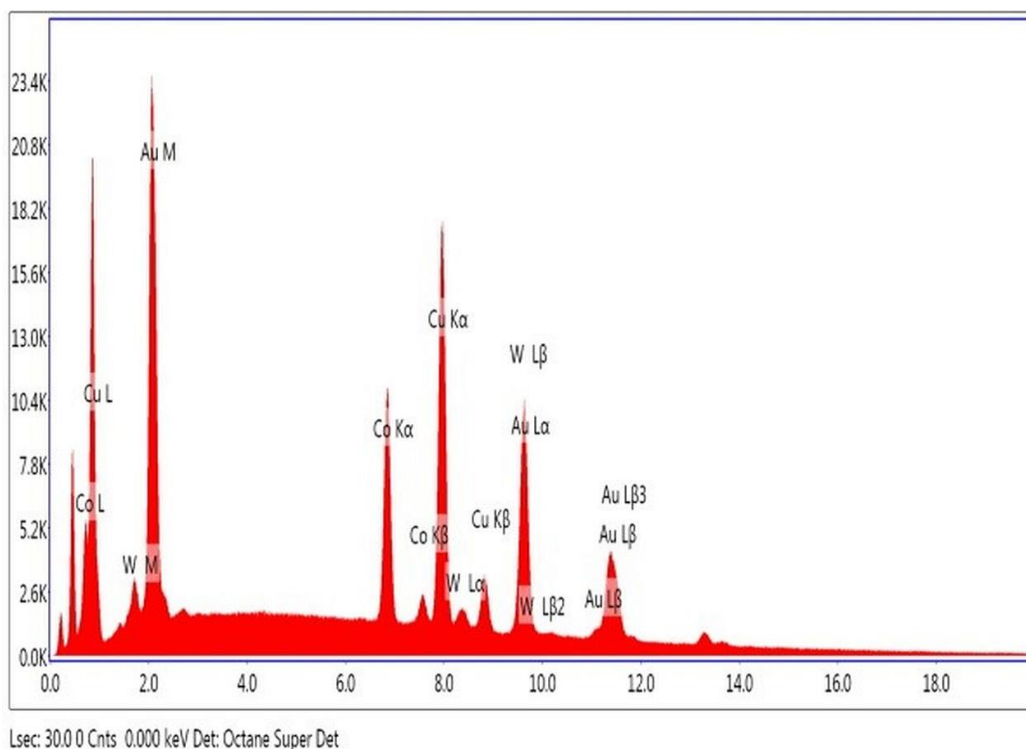


**Figure 9.** EDS spectra for the CoW/Cu/CoW composite obtained from Electrolyte I (IA and IB), without the CMF.

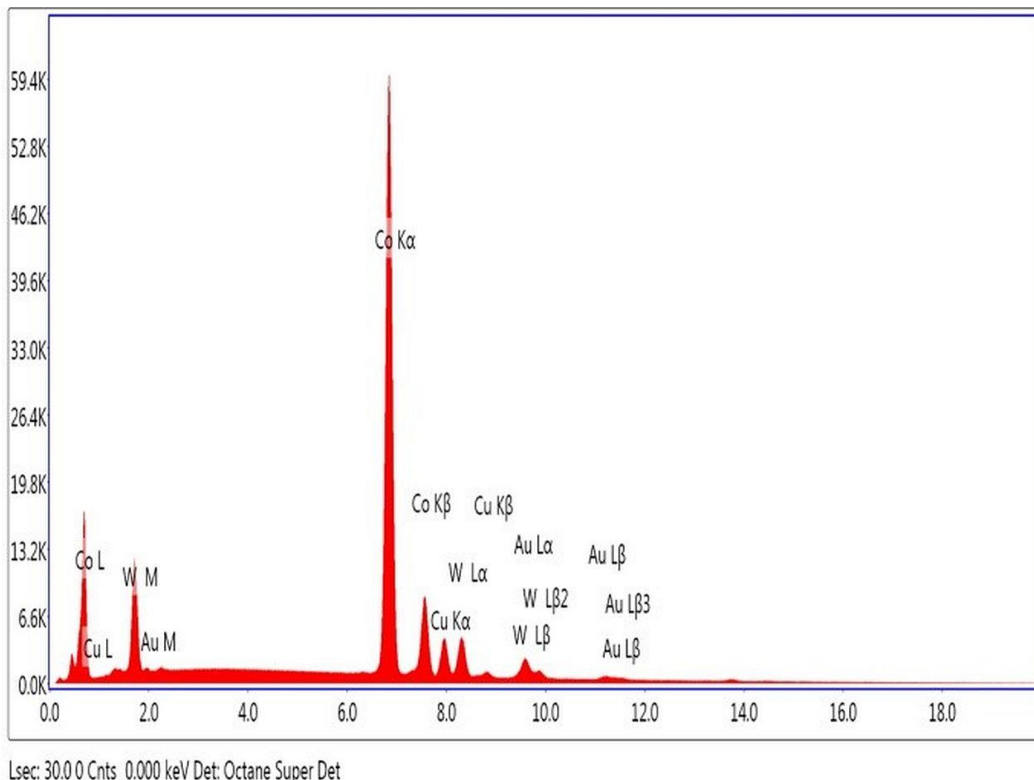


**Figure 10.** EDS spectra for the CoW/Cu/CoW composite obtained from Electrolyte I (IA and IB), under the influence of CMF.

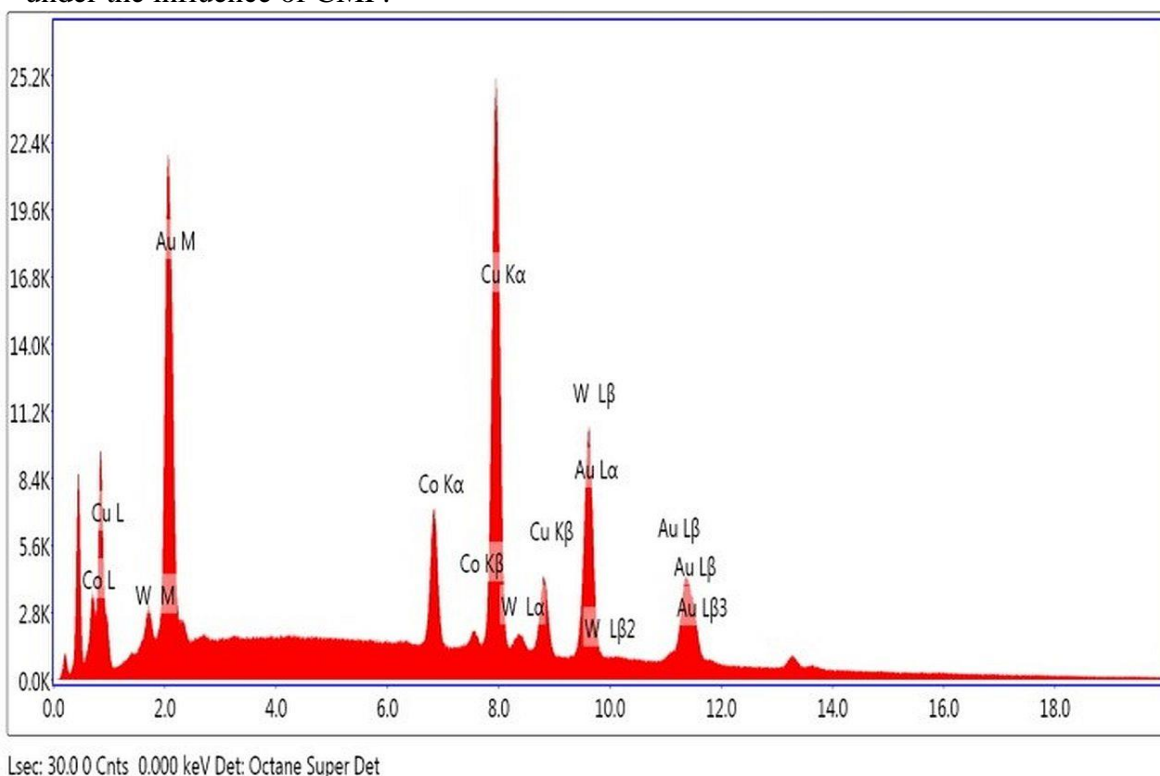


**Figure 11.** EDS spectra for the CoW/Cu/CoW composite obtained from Electrolyte II, without the CMF

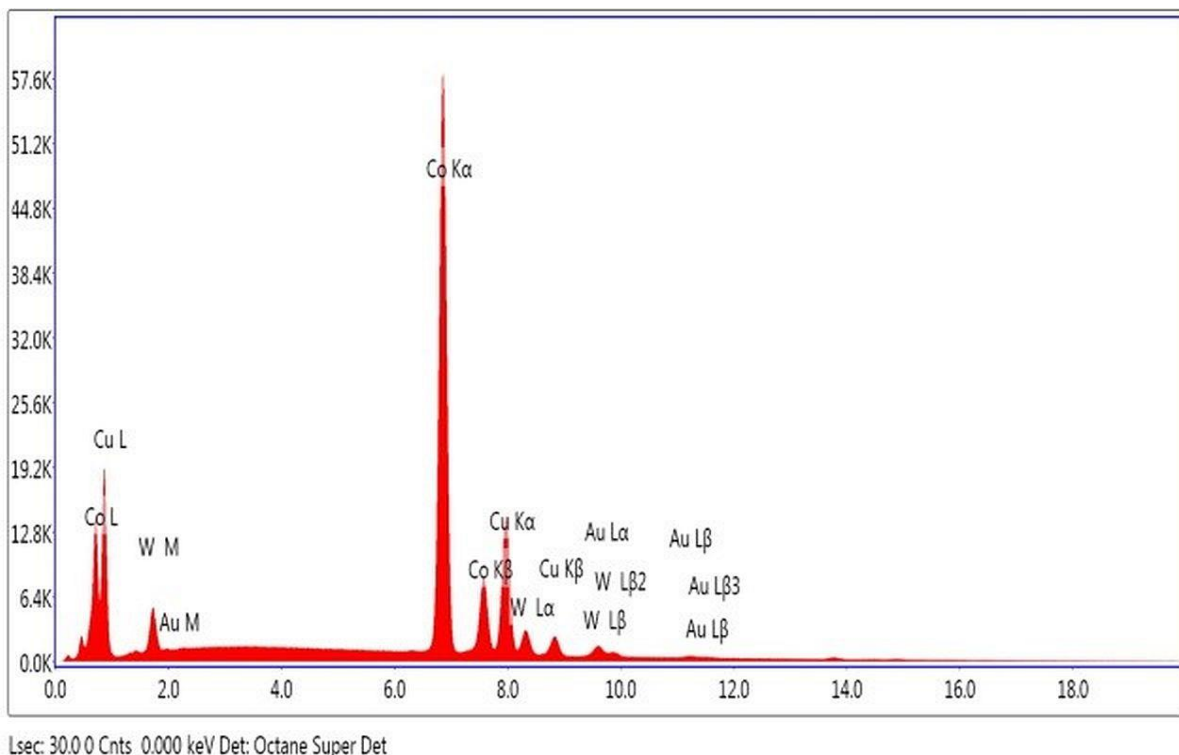


**Figure 12.** EDS spectra for the CoW/Cu/CoW composite obtained from Electrolyte II, under the influence of CMF

The composite area deposited in constant magnetic field has a lower number of fractures. In addition, the fractures on the surface of the material are much smaller. The influence of CMF on the chemical composition was examined on the tested composites using EDS.

Figures 9 – 12 represent EDS spectra of the CoW/Cu/CoW composite, obtained from Electrolyte I (IA and IB) and Electrolyte II, in the CMF and without the magnetic field.

**Table 2.** Percentage composition of CoW/Cu/CoW composite obtained from Electrolyte I (IA and IB) and consecutively from Electrolyte II.

Element	B = 0 T	B = 1 T
Composite (CoW/Cu/CoW) obtained from Electrolyte I (IA and IB)		
Co	22.66% weight	74.54% weight
Cu	62.28% weight	7.98% weight
W	10.06% weight	17.48% weight
Composite (CoW/Cu/CoW) obtained from Electrolyte II		
Co	14.27% weight.	64.55% weight.
Cu	78.38% weight.	25.08% weight.
W	7.35% weight.	10.37% weight.

The energy values corresponding to the lines characteristic of the test spectrum made it possible to identify the type of elements. Such identification uniquely identified the elemental composition of the test composite. The size of the area under the peak intensity allowed for the

estimation of the percentage at which the element occurs in the area penetrated by the electron beam. The calculation of the percentage of elements in the analyzed volume of the sample was performed using a computer program, using the ZAF type correction. This enabled to achieve the measurement accuracy of 1% quantitative content of the element present in the tested sample. The results of the quantitative analysis of the CoW/Cu/CoW composite, obtained from Electrolyte I (IA and IB) and Electrolyte II are provided in Table 2.

The results show that the impact of CMF causes changes in the chemical composition of the material. The presence of CMF during the electrodeposition leads to an increase in the content of the ferromagnetic component (CoW) and a decrease in the amount of the diamagnetic component (Cu). These results indicate that the rate of deposition of the more noble metal (Cu in this case) is inhibited, and the less noble layer (CoW) is deposited more quickly under the influence of CMF. Similar results were presented, among others, by Aaoubou and Msellak [17]. Fricoteaux and Rousse also wrote [27] that: throughout these investigations on the Ni–Fe alloy compositions, we have studied the nickel percentage inside deposit versus the polarization. The evolution of the nickel proportion can be stand out in three parts. The first one, for low polarization, fits with a decrease of nickel percentage, the second one with an increase of this percentage and for high polarization a stabilization of the composition is obtained. In consequence, two different polarizations allow obtaining the same alloy composition.

### 3.3. Giant Magnetoresistance (GMR)

In the study, the metallic CoW/Cu/CoW composite was deposited, as well as the reference Fe/Cr/Fe with high magnetoresistance. Change in resistance of the material under the influence of an external magnetic field (giant magnetoresistance) takes place under the spin scattering of conduction electrons at each superlattice layer, depending on the relative orientation of the magnetization directions. In the case where  $B = 0$ , the directions of magnetization of ferromagnetic layers are characterized by an anti-parallel arrangement, which results in a maximum resistance of the material. When  $B > 0$ , the arrangement directions of spins of electrons result in minimal resistance of the material due to the lower energy barrier (less scattering) (Figure 13).

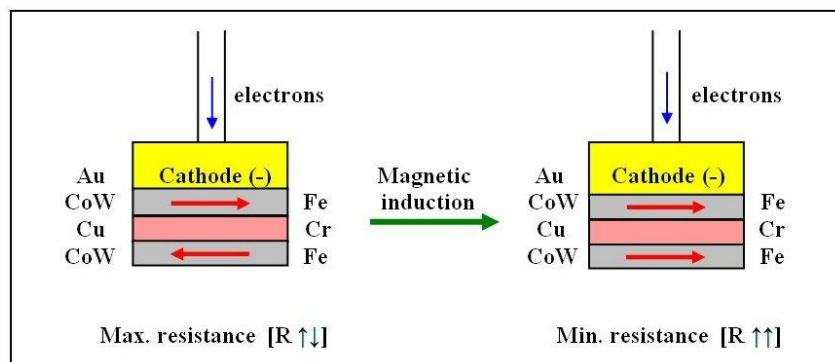


**Figure 13.** Schematic diagram of the formed material layers, direction of the electrons flow, direction of the magnetic induction vector, and direction of the electron spins in the ferromagnetic layers, before and after exposure to constant magnetic field.

Analysis of the resistance change in the material deposited on the Au electrode, based on the anodic current in the CMF and without any magnetic field was considered as the sum of the effect of the constant magnetic field on the oxidation process, and the change in resistance of the material (Figure 14).

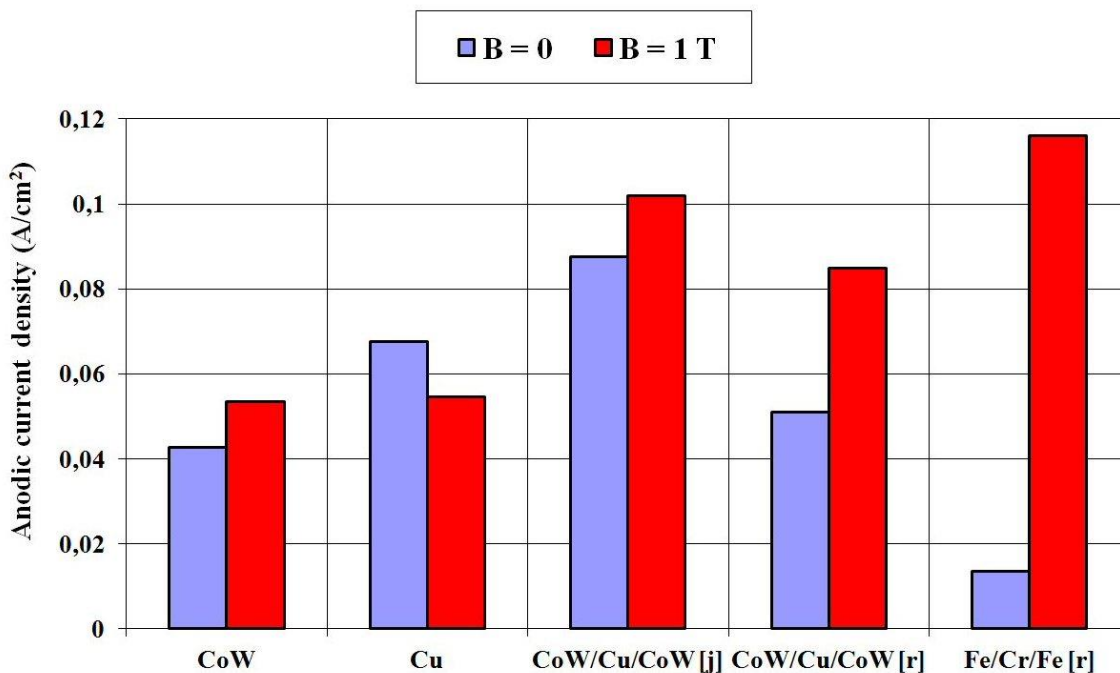


**Figure 14.** Anodic current density values ( $j_a$ ) in the processes of oxidation of materials (alloy, metal and composite) in and without the presence of constant magnetic field, where: CoW/Cu/CoW [j] denotes the CoW/Cu/CoW composite obtained from Electrolyte II; CoW/Cu/CoW [r] the CoW/Cu/CoW composite obtained consecutively from Electrolyte I (IA and IB).

Thus, the percentage resistance changes in constant magnetic field of magnetic resistance  $B = 1$  T can be estimated. Using the Ohm law formula:

$$R = \frac{U}{i} = \text{cons.} \quad \text{and the} \quad \Delta R = \left( \frac{R_0 - R_B}{R_0} \right) \cdot 100\% \quad \text{equation, the resistance changes increased by the}$$

effect of constant magnetic field on the electrooxidation process can be calculated (Table 3).

**Table 3.** Changes in the resistance of the Fe/Cr/Fe and CoW/Cu/CoW composites, where:  $R_0$  = composite resistance without constant magnetic field,  $R_B$  = composite resistance in constant magnetic field.

$R_0$ [ $\Omega$ ]	$R_B$ [ $\Omega$ ]	$\Delta R$ [%]
Composite Fe/Cr/Fe		
8.444	0.966	88.56
Composite (CoW/Cu/CoW) obtained from Electrolyte I (IA and IB)		
0.310	0.207	33.23
Composite (CoW/Cu/CoW) obtained from Electrolyte II		
0.184	0.157	14.67

#### 4. CONCLUSIONS

Based on the results of research and analysis, the following conclusions have been drawn:

- i. At a selected sweep rate, there is an increase of peak values of electrooxidation anode current density for CoW/Cu/CoW composite layer in a constant magnetic field.
- ii. In the constant magnetic field, the shift in values occurs towards a more positive oxidation potential of the CoW/Cu/CoW composite layers. In consequence, the potential difference between the reduction potential and oxidation potential increases, which causes an increase in the degree of irreversibility of the process.
- iii. Changes of value were determined between the current densities ( $\Delta j$ ) and between potentials ( $\Delta U$ ), coming to the conclusion that ( $\Delta U$ ) and ( $\Delta j$ ) for diamagnetics decrease depending on the increase in the of the magnetic induction ( $B$ ) value, whereas they increase for ferromagnetics and paramagnetics.
- iv. Resistance decreases in the CMF by 88.56% for Fe/Cr/Fe, 33.23% for CoW/Cu/CoW [obtained from Electrolyte I (IA and IB)], 14.67% for CoW/Cu/CoW (obtained from Electrolyte II).
- v. The influence of CMF changes the surface morphology. The CoW/Cu/CoW composite deposited in CMF is characterized by its smoother surface.
- vi. The influence of CMF increases the corrosion resistance of the material due to reduced internal stress of the material.
- vii. The presence of CMF changes the chemical composition of the test material. There is an increase of the ferromagnetic component, and a decrease of the diamagnetic component.

#### ACKNOWLEDGEMENTS

This work was supported by the University of Lodz.

#### References

1. A. Tokarz, A. Wolkenber and M. Kęsik, *Composites*, 2 (2003) 85.
2. M. Kowalewska and M. Trzaska, *Composites*, 5 (2004) 36.
3. E. Chassaing, *J. Electrochem. Soc.*, 144 (1997) 328.
4. E. Gomez, S. Pane and E. Valles, *Electrochim. Acta*, 51 (2005) 146.
5. A. Cziraki, *Thin Solid Films*, 433 (2003) 237.
6. G. Nabiyouni, W. Schwarzacher, Z. Rolik and I. Bakonyi, *J. Magn. Magn. Mater.*, 253 (2002) 77.
7. M. Zieliński and E. Miękoś, *J. Appl. Electrochem.*, 38 (2008) 1771.
8. S.M. Mayanna, L. Ramesh and B.N. Maruthi, *J. Mater. Sci. Lett.*, 16 (1997) 1305.
9. W. Szmaja, W. Kozłowski, K. Polański, J. Balcerski, M. Cichomski, J. Grobelny, M. Zieliński and E. Miękoś, *Mater. Chem. Phys.*, 132 (2012) 1060.
10. J.A. Koza, M. Uhlemann, A. Gebert and L. Schultz, *Electrochim. Acta*, 53 (2008) 5344.
11. N. Tsyntsaru, H. Cesiulis, E. Pellicer, J.-P. Celis and J. Sort, *Electrochim. Acta*, 104 (2013) 94.
12. G. Hinds, J.M.D. Coey and M.E.G. Lyons, *Electrochem. Commun.*, 3 (2001) 215.
13. D. Fernandez and J.M.D. Coey, *Electrochem. Commun.*, 11 (2009) 379.

14. K. Msellak, J.-P. Chopart, O. Jbara, O. Aaboubi and J. Amblard, *J. Magn. Magn. Mater.*, 281 (2004) 294.
15. M. Zieliński, *Mater. Chem. Phys.*, 141 (2013) 370.
16. M. Zieliński, *Int. J. Electrochem. Sci.*, 8 (2013) 12192.
17. O. Aaboubi and K. Msellak, *Appl. Surf. Sci.*, 396 (2017) 375.
18. M. Zieliński, E. Miękoś, D. Szczukocki, R. Dałkowski, A. Leniart, B. Krawczyk and R. Juszcak, *Int. J. Electrochem. Sci.*, 10 (2014) 4146.
19. H. Matsushima, T. Nohira, I. Mogi and Y. Ito, *Surf. Coat. Tech.*, 179 (2004) 245.
20. C. O'Reilly, G. Hinds and J.M.D. Coey, *J. Electrochem. Soc.*, 148 (2001) 674.
21. T.Z. Fahidy, *J. Appl. Electrochem.*, 13 (1983) 553.
22. L.M.A. Moznon and J.M.D. Coey, *Electrochem. Commun.*, 42 (2014) 38.
23. A. Krause, M. Uhlemann, A. Gebert and L. Schultz, *Electrochim. Acta*, 49 (2004) 4127.
24. O. Lioubashevski, E. Katz and I. Willner, *J. Phys. Chem. B*, 108 (2004) 5778.
25. M. Ebadi, W.J. Basirun, Y. Alias, M. Mahmoudian and S. Leng, *Mater. Charact.*, 66 (2012) 46.
26. S. Olvera, E.M. Arce Estrada, J. Sanchez-Marcos, F.J. Palomares, L. Vazquez and P. Herrasti, *Mater. Charact.* 105 (2015) 136.
27. P. Fricoteaux and C. Rousse, *J. Electroanal. Chem.*, 612 (2008) 9.

© 2018 The Authors. Published by ESG ([www.electrochemsci.org](http://www.electrochemsci.org)). This article is an open access article distributed under the terms and conditions of the Creative Commons Attribution license (<http://creativecommons.org/licenses/by/4.0/>).